β-Turn Preferences Induced by 2,3-Methanophenylalanine Chirality†

A. I. Jiménez,‡,⊥ C. Cativiela,§ A. Aubry,|| and M. Marraud*,‡

Contribution from the Laboratory of Macromolecular Physical Chemistry, UMR-7568 CNRS-INPL, ENSIC, BP 451, 54001 Nancy, France, Department of Organic Chemistry, ICMA, CSIC-University of Zaragoza, E-50009 Zaragoza, Spain, and Laboratory of Crystallography and Modeling of Mineral and Biological Materials, ESA-7036, University Henri Poincaré of Nancy, BP 236, 54509 Vandoeuvre, France

Received March 5, 1998. Revised Manuscript Received June 29, 1998

Abstract: The model dipeptides RCO-L-Pro-c_3Phe-NHMe, where c_3Phe stands for each of the four cyclopropane analogues of phenylalanine (2,3-methanophenylalanine), have been studied in solution by using ^{1}H NMR and FT-IR spectroscopy and in the solid state by using X-ray diffraction. The conformational behavior of these compounds has been compared to that of the analogous Ac_3c and L- or D-Phe-containing dipeptides. When associated to proline, the cyclopropane residues in the so-called $i + 2$ position exhibit a marked tendency to β-folding in solution, even in DMSO. The type II β-turn is generally favored, but the βI/βII-turn ratio depends both on the experimental conditions (solvent, solution, or solid state) and on the chirality of the c_3Phe moiety, which rigidly fixes the orientation of the phenyl ring with respect to the peptide backbone. The (2*S*,3*S*)c_3Phe residue, analogous to L-Phe with the χ^1 angle constrained to about 0°, is the most propitious to βI-folding in the $i + 2$ position of a putative β-turn.

The biological effects mediated by peptides greatly depend on their conformational properties, which are of primary importance in molecular recognition steps. However, small and medium-sized peptides often exhibit a conformational flexibility that gives them the possibility of interacting with different receptors, thus presenting a multiple biological activity. The stabilization of particular conformational features by the introduction of geometrical constraints may be of major interest for the establishment of structure−activity relationships.

Structural restrictions can be induced in different ways, with one of the most efficient being the incorporation of nonproteinogenic α-amino acids with defined conformational preferences.[1] Among such methods, α-alkylation has proven to be valuable in the construction of peptides with specific secondary structures, and the resulting conformation depends on the type of α-alkylation.[2] Thus, α-amino isobutyric acid (Aib) induces 3_{10}- or α-helices depending on the number of Aib residues,[3] whereas larger linear substituents in open α,α-dialkylated residues seem to favor extended structures.[2a−d] Folded conformations are often observed in peptides containing 1-aminocycloalkanecarboxylic acids.[2a−e,4] However, very little work has been devoted to the incorporation of chiral derivatives of α-amino acids other than α-methylated compounds.[5]

It should also be noted that some particular side chains are directly involved in molecular contacts and are therefore strictly required for adequate peptide-receptor recognition and binding affinity. Moreover, statistical analysis of the crystallized proteins reveals that local structural motifs are often the consequence of side chain/main chain interactions.[6] For example, the Asx-turn is characterized by a hydrogen bond, which closes a 10-membered cycle, between a peptide NH and an Asn-C$^\gamma$O or Asp-C$^\gamma$O$_2^-$ two residues ahead and requires a particular orientation of the Asn or Asp side chain.[7] It then appears that, due to either steric hindrance or the occurrence of a defined interaction, the conformation of a peptide chain and the orientation of the side substituents are not independent parameters. For these reasons, the introduction of conformational constraints to force the side substituents to adopt a definite

† Abbreviations: Standard abbreviations as recommended by the ACS and the IUPAC-IUB Commission have been used. Ac_3c, 1-aminocyclopropanecarboxylic acid; Boc, *tert*-butyloxycarbonyl; c_3Phe, 2,3-methanophenylalanine; HOHAHA, homonuclear Hartmann−Hahn spectroscopy; NMM, *N*-methylmorpholine; PE, petroleum ether; Piv, pivaloyl (*tert*-butylcarbonyl); TFA, trifluoroacetic acid; Z, benzyloxycarbonyl.

‡ Laboratory of Macromolecular Physical Chemistry, ENSIC-INPL.

§ Department of Organic Chemistry, University of Zaragoza.

|| Laboratory of Crystallography and Modeling of Mineral and Biological Materials, University Henri Poincaré of Nancy.

⊥ Present address: Department of Organic Chemistry, University of Zaragoza.

(1) Hruby, V. J.; Li, G.; Haskell-Luevano, C.; Shenderovich, M. *Biopolymers* **1997**, *43*, 219−266.

(2) (a) Benedetti, E. *Biopolymers* **1996**, *40*, 3−44. (b) Di Blasio, B.; Pavone, V.; Lombardi, A.; Pedone, C.; Benedetti, E. *Biopolymers* **1993**, *33*, 1037−1049. (c) Toniolo, C.; Benedetti, E. *Macromolecules* **1991**, *24*, 4004−4009. (d) Toniolo, C. *Janssen Chim. Acta* **1993**, *11*, 10−16. (e) Toniolo, C.; Crisma, M.; Formaggio, F.; Benedetti, E.; Santini, A.; Iacovino, R.; Saviano, M.; Di Blasio, B.; Pedone, C.; Kamphuis, J. *Biopolymers* **1996**, *40*, 519−522. (f) Toniolo, C.; Crisma, M.; Formaggio, F.; Valle G.; Cavicchioni, G.; Precigoux, G.; Aubry, A.; Kamphuis, J. *Biopolymers* **1993**, *33*, 1061−1072. (g) Toniolo, C.; Crisma, M.; Formaggio, F.; Polese, A.; Doi, M.; Ishida, T.; Mossel, E.; Broxterman, Q.; Kamphuis, J. *Biopolymers* **1996**, *40*, 523−527.

(3) Karle, I. L.; Balaram, P. *Biochemistry* **1990**, *29*, 6747−6756.

(4) (a) Gatos, M.; Formaggio, F.; Crisma, M.; Toniolo, C.; Bonora, G. M.; Benedetti, E.; Di Blasio, B.; Iacovino, R.; Santini, A.; Saviano, M.; Kamphuis, J. *J. Pept. Sci.* **1997**, *3*, 110−122. (b) Gatos, M.; Formaggio, F.; Crisma, M.; Valle, G.; Toniolo, C.; Bonora, G. M.; Saviano, M.; Iacovino, R.; Menchise, V.; Galdiero, S.; Pedone, C.; Benedetti, E. *J. Pept. Sci.* **1997**, *3*, 367−382. (c) Moretto, V.; Formaggio, F.; Crisma, M.; Bonora, G. M.; Toniolo, C.; Benedetti, E.; Santini, A.; Saviano, M.; Di Blasio, B.; Pedone, C. *J. Pept. Sci.* **1996**, *2*, 14−27. (d) Benedetti, E.; Di Blasio, B.; Iacovino, R.; Menchise, V.; Saviano, M.; Pedone, C.; Bonora, G. M.; Ettorre, A.; Graci, L.; Formaggio, F.; Crisma, M.; Valle, G.; Toniolo, C. *J. Chem. Soc., Perkin Trans. 2* **1997**, 2023−2032.

(5) (a) Doi, M.; Ishida, T.; Polese, A.; Formaggio, F.; Crisma, M.; Toniolo, C.; Broxterman, Q. B.; Kamphuis, J. *Pept. Res.* **1995**, *8*, 294−297. (b) Formaggio, F.; Pantano, M.; Crisma, M.; Bonora, G. M.; Toniolo, C.; Kamphuis, J. *J. Chem. Soc., Perkin Trans. 2* **1995**, 1097−1101.

(6) Baker, E.; Hubbard, R. E. *Prog. Biophys. Mol. Biol.* **1984**, *44*, 97−180.

(7) Abbadi, A.; Mcharfi, M.; Aubry, A.; Prémilat, S.; Boussard, G.; Marraud, M. *J. Am. Chem. Soc.* **1991**, *113*, 2729−2735.

S0002-7863(98)00743-4 CCC: $15.00
Published on Web 09/05/1998

orientation, without necessarily modifying their chemical nature, is of valuable interest.[1]

Despite their potential utility, the conformational consequences of selectively oriented side chains remain almost unexplored.[1] Cyclopropane (or 2,3-methano) amino acid analogues are particularly attractive from this point of view. In addition to the restrictions imposed by α,α-disubstitution, the rigidity of the structure forces the side chain to adopt a well-defined orientation with respect to the backbone, and this orientation is different for each diastereoisomer. Evidence of this interest is provided by the effort devoted during recent years to the synthesis of these derivatives.[8] Stereoselective procedures for the preparation of cyclopropane analogues of methionine,[9] phenylalanine,[10] leucine,[11] arginine,[12] proline,[13] aspartic acid,[14] glutamic acid,[15] and glutamine[16] have recently been reported. Although 1-aminocyclopropanecarboxylic acid has been inserted into a certain number of peptides,[2a−d,17] there are only a few examples concerning substituted cyclopropane analogues of proteinogenic amino acids. 2,3-Methanophenylalanine has been incorporated into aspartame,[18] enkephalin,[19] and substance P.[20] Various di- and tripeptides including 2,3-methanoaspartic acid have been synthesized.[21] Theoretical and spectroscopic analyses of some 2,3-methanomethionine- or 2,3-methanoarginine-containing peptides have been reported.[22,23] The crystal molecular structure of only one dipeptide containing 2,3-methanophenylalanine has been described.[24]

To study the influence of the side chain orientation on the folding mode of a peptide, we have prepared the model dipeptides RCO-L-Pro-Xaa-NHMe (RCO = Z, Boc, or Piv), where Xaa represents each of the four 2,3-methanophenylalanine diastereoisomers (denoted as c_3Phe in the following text), 1-aminocyclopropanecarboxylic acid (denoted as Ac_3c), and L- or D-phenylalanine. The two dipeptides incorporating phenylalanine have already been shown to adopt the type II β-turn in the solid state and the βI- or βII-turn structure, depending on their stereochemistry, in CH_2Cl_2 solution.[25] We have applied IR and ^{1}H NMR spectroscopy to the structural analysis of the c_3Phe derivatives in solution and compared their behavior to that of the Ac_3c- and Phe-containing dipeptides. Three of the four c_3Phe diastereoisomers gave crystallized dipeptides, which have been investigated by X-ray diffraction. Preliminary results have recently been published elsewhere.[26]

Experimental Section

Synthesis. The derivatives that have been synthesized are shown in Table 1 with their abbreviated codes. Amino esters *cis*-**8** and *trans*-**8** (racemic form), as well as **9**, were obtained by acid hydrolysis of their respective diphenylmethylene imino esters (Figure 1), which were prepared following previously reported procedures.[28,29] The synthesis of the four diastereoisomers **1**−**4** is presented in Figure 2. *cis*-**8** and *trans*-**8** were coupled to *N*-*tert*-butyloxycarbonyl-L-proline by the classical mixed anhydride method using isobutyl chloroformate as a coupling agent[30] to give **1b**−**4b**. Subsequent treatment of these compounds with methylamine in methanolic solution afforded the corresponding methylamides **1a**−**4a** in good yields. Due to steric hindrance arising from α,α-disubstitution and the presence of the phenyl group, the time required for completion of the reactions was in most cases significantly longer than that under the standard conditions. The *cis* diastereoisomeric esters **1b** and **2b**, and the *trans* diastereoisomeric amides **3a** and **4a**, were separated by column chromatography on silica gel. The Boc group in **1a**−**4a** was removed by treatment with trifluoroacetic acid, and the amino group was acylated with pivaloyl chloride to give **1**−**4**. At this stage, only **1** and **3a** gave single crystals suitable for X-ray diffraction experiments. L-Proline was taken as a reference, and the resolution of the crystal structures revealed the absolute configuration of the c_3Phe residue to be (2*R*,3*R*) in series **1** and (2*R*,3*S*) in series **3**. From these results, the stereochemistry of the cyclopropane moiety in series **2** and **4** could be established as (2*S*,3*S*) and (2*S*,3*R*), respectively (Figure 3). This assignment was verified with the crystal structure of **2c**, obtained from **2a** by changing the Boc group

(8) (a) Stammer, C. H. *Tetrahedron* **1990**, *46*, 2231−2254. (b) Alami, A.; Calmes, M.; Daunis, J.; Jacquier, R. *Bull. Soc. Chim. Fr.* **1993**, *130*, 5−24. (c) Burgess, K.; Ho, K. K.; Moye-Sherman, D. *Synlett* **1994**, 575−583.

(9) Burgess K., Ke C.-Y., *Synthesis* **1996**, 1463−1467.

(10) (a) Williams, R. M.; Fegley, G. J. *J. Am. Chem. Soc.* **1991**, *113*, 8796−8806. (b) Williams, R. M.; Fegley, G. J. *J. Org. Chem.* **1993**, *58*, 6933−6935. (c) Davies, H. M. L.; Bruzinski, P. R.; Lake, D. H.; Kong N.; Fall, M. J. *J. Am. Chem. Soc.* **1996**, *118*, 6897−6907. (d) Davies, H. M. L.; Huby, N. J. S.; Cantrell, W. R.; Olive J. L. *J. Am. Chem. Soc.* **1993**, *115*, 9468−9479. (e) Alcaraz, C.; Fernández, M. D.; de Frutos, M. P.; Marco, J. L.; Bernabé, M. *Tetrahedron* **1994**, *50*, 12443−12456.

(11) Burgess, K.; Li, W. *Tetrahedron Lett.* **1995**, *36*, 2725−2728.

(12) (a) Burgess, K.; Ho, K.-K. *Tetrahedron Lett.* **1992**, *33*, 5677−5680. (b) Burgess, K.; Lim, D.; Ho, K.-K.; Ke, C.-Y. *J. Org. Chem.* **1994**, *59*, 2179−2185.

(13) Hercouet, A.; Bessières, B.; Le Corre, M. *Tetrahedron: Asymmetry* **1996**, *7*, 1267−1268.

(14) Jiménez, J. M.; Rifé, J.; Ortuño, R. M. *Tetrahedron: Asymmetry* **1996**, *7*, 537−558.

(15) Jiménez, J. M.; Ortuño, R. M. *Tetrahedron: Asymmetry* **1996**, *7*, 3203−3208.

(16) Burgess, K.; Lim, D. Y. *Tetrahedron Lett.* **1995**, *36*, 7815−7818.

(17) (a) Zhu, Y.-F.; Yamazaki, T.; Tsang, J. W.; Lok, S.; Goodman, M. *J. Org. Chem.* **1992**, *57*, 1074−1081. (b) Fabiano, N.; Valle, G.; Crisma, M.; Toniolo, C.; Saviano, M.; Lombardi, A.; Isernia, C.; Pavone, V.; Di Blasio, B.; Pedone, C.; Benedetti, E. *Int. J. Pept. Protein Res.* **1993**, *42*, 459−465. (c) Benedetti, E.; Di Blasio, B.; Pavone, V.; Pedone, C.; Santini, A.; Barone, V.; Fraternali, F.; Lelj, F.; Bavoso, A.; Crisma, M.; Toniolo, C. *Int. J. Biol. Macromol.* **1989**, *11*, 353−360. (d) Valle, G.; Crisma, M.; Toniolo, C.; Holt, E. M.; Tamura, M.; Bland, J.; Stammer, C. H. *Int. J. Pept. Protein Res.* **1989**, *34*, 56−65. (e) Crisma, M.; Bonora, G. M.; Toniolo, C.; Barone, V.; Benedetti, E.; Di Blasio, B.; Pavone, V.; Pedone, C.; Santini, A.; Fraternali, F.; Bavoso, A.; Lelj, F. *Int. J. Biol. Macromol.* **1989**, *11*, 345−352. (f) Barone, V.; Fraternali, F.; Cristinziano, P. L.; Lelj, F.; Rosa, A. *Biopolymers* **1988**, *27*, 1673−1685. (g) Benedetti, E.; Di Blasio, B.; Pavone, V.; Pedone, C.; Santini, A.; Crisma, M.; Valle, G.; Toniolo, C. *Biopolymers* **1989**, *28*, 175−184. (h) Mapelli, C.; Newton, M. G.; Ringold, C. E.; Stammer, C. H. *Int. J. Pept. Protein Res.* **1987**, *30*, 498−510.

(18) Mapelli, C.; Stammer, C. H.; Look, S.; Mierke, D. F.; Goodman, M. *Int. J. Pept. Protein Res.* **1988**, *32*, 484−495.

(19) (a) Mapelli, C.; Kimura, H.; Stammer, C. H. *Int. J. Pept. Protein Res.* **1986**, *28*, 347−359. (b) Shimohigashi, Y.; Costa, T.; Pfeiffer, A.; Herz, A.; Kimura, H.; Stammer, C. H. *FEBS Lett.* **1987**, *222*, 71−74. (c) Shimohigashi, Y.; Takano, Y.; Kamiya, H.; Costa, T.; Herz, A.; Stammer, C. H. *FEBS Lett.* **1988**, *233*, 289−293.

(20) Déry, O.; Josien, H.; Grassi, J.; Chassaing, G.; Couraud, J. Y.; Lavielle, S. *Biopolymers* **1996**, *39*, 67−74.

(21) Godier-Marc, E.; Aitken, D. J.; Husson, H. P. *Tetrahedron Lett.* **1997**, *38*, 4065−4068.

(22) (a) Burgess, K.; Ho, K.-K.; Pettitt, B. M. *J. Am. Chem. Soc.* **1994**, *116*, 799−800. (b) Burgess, K.; Ho, K.-K.; Pettitt, B. M. *J. Am. Chem. Soc.* **1995**, *117*, 54−65. (c) Burgess, K.; Ho, K.-K.; Pal, B. *J. Am. Chem. Soc.* **1995**, *117*, 3808−3819. (d) Burgess, K.; Ke, C.-Y. *J. Org. Chem.* **1996**, *61*, 8627−8631. (e) Burgess, K.; Ke, C.-Y. *J. Pept. Res.* **1997**, *49*, 201−209. (f) Malin, D. H.; Payza, K.; Lake, R.; Corriere, L. S.; Benson, T. M.; Smith, D. A.; Kelley, R. S.; Ho, K.-K.; Burgess, K. *Peptides* **1993**, *14*, 47−51. (g) Malin, D. H.; Lake, R.; Payza, K.; Corriere, L. S.; Benson, T. M.; Garber, T. L.; Waller, M. L.; Luu, T.-A.; Kelley, R. S.; Smith, D. A.; Ho, K.-K.; Burgess, K. *Peptides* **1993**, *14*, 731−734.

(23) Lim, D.; Burgess, K. *J. Am. Chem. Soc.* **1997**, *119*, 9632−9640.

(24) Varughese, K. I.; Wang, C. H.; Kimura, H.; Stammer, C. H. *Int. J. Pept. Protein Res.* **1988**, *31*, 299−300. Due to the erroneous stereochemistry of the L-Leu residue, the chirality of the 2,3-methanophenylalanine must be changed into (2*S*,3*R*).

(25) Aubry, A.; Cung, M. T.; Marraud, M. *J. Am. Chem. Soc.* **1985**, *107*, 7, 7640−7647.

(26) Jiménez, A. I.; Vanderesse, R.; Marraud, M.; Aubry, A.; Cativiela, C. *Tetrahedron Lett.* **1997**, *38*, 7559−7562.

(27) Bardi, R.; Piazzesi, A. M.; Toniolo, C.; Sen, N.; Balaram, H.; Balaram, P. *Acta Crystallogr., Sect. C* **1988**, *44*, 1972−1976.

(28) Cativiela, C.; Díaz-de-Villegas, M. D.; Jiménez, A. I. *Tetrahedron* **1994**, *50*, 9157−9166.

(29) Cativiela, C.; Díaz-de-Villegas, M. D.; Jiménez, A. I. *Synth. Commun.* **1992**, *22*, 2955−2963.

(30) Bodanszky, M.; Bodanszky, A. *The Practice of Peptide Synthesis*; Springer-Verlag: Berlin, Germany, 1994.

Table 1. Synthesized Dipeptides with Configurations and Codes

Xaa residue	c_3Phe					Phe	
absolute configuration peptide nomenclature[a]	(2*R*,3*R*) *cis*, D	(2*S*,3*S*) *cis*, L	(2*R*,3*S*) *trans*, D	(2*S*,3*R*) *trans*, L	Ac_3c[c]	(*S*) L	(*R*) D
Piv-L-Pro-Xaa-NHMe	**1**[b]	**2**	**3**	**4**	**5**	**6**[c]	**7**[d]
Boc-L-Pro-Xaa-NHMe	**1a**	**2a**	**3a**[b]	**4a**	**5a**	**6a**	**7a**
Boc-L-Pro-Xaa-OMe	**1b**	**2b**	**3b**	**4b**	**5b**		
Z-L-Pro-Xaa-NHMe		**2c**[b]					

[a] The peptide nomenclature is indicated for comparison of the 2,3-methanophenylalanine configuration with that of the Phe residue. The disposition of the phenyl ring with reference to the nitrogen is denoted by *cis* and *trans*. [b] The crystal molecular structure of this derivative has been solved (this work). [c] The crystal molecular structure of this derivative has been solved.[25] [d] The crystal molecular structure of this derivative has been solved.[27]

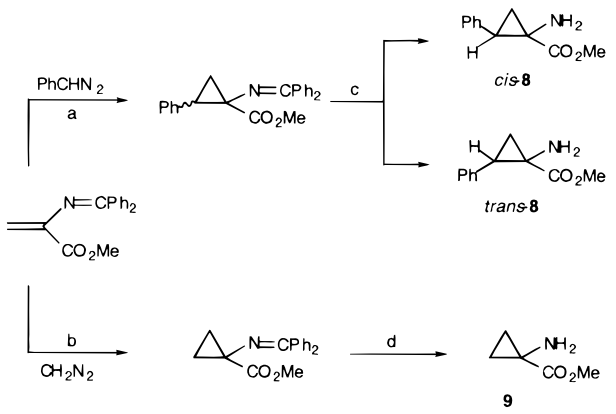

Figure 1. Synthesis of the starting cyclopropane amino esters **8** and **9**. Conditions: (a) Ref 28. (b) Ref 29. (c) 1 N HCl/CH_2Cl_2, rt 24 h; column chromatography (eluent AcOEt/CH_2Cl_2 1/1), R_f 0.60 (*cis*-**8**), 0.31 (*trans*-**8**); overall yield: 98%. (d) 0.5 N HCl/CH_2Cl_2, rt overnight; yield: 89%.

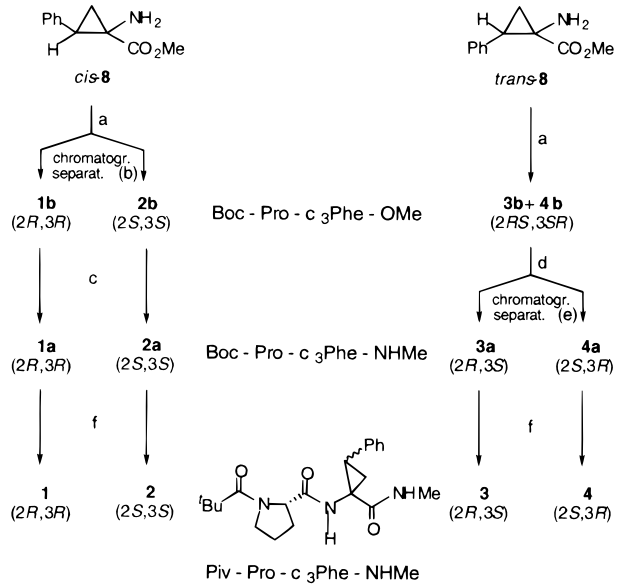

Figure 2. Synthesis of the four diastereoisomeric dipeptides **1**−**4**. Conditions: (a) Boc-L-Pro-OH/*i*-BuOCOCl/NMM/THF, −15 °C 4 h, rt overnight; yield > 95%. (b) Eluent AcOEt/PE 3/2; R_f 0.44 (**1b**), 0.37 (**2b**). (c) 8m $MeNH_2$/MeOH, rt 24 h; yield >95%. (d) 8 M $MeNH_2$/MeOH, rt 8 d; yield >90%. (e) Eluent AcOEt/CH_2Cl_2, 1/1; R_f 0.33 (**3a**), 0.30 (**4a**). (f) 1: TFA/CH_2Cl_2, 2/3, rt 1 h; 2: *t*-BuCOCl/NMM/$CHCl_3$, 0 °C 2 h, rt overnight; yield >92%.

into the Z one. Unfortunately, all efforts to crystallize derivatives in series **4** were unsuccessful. The Ac_3c-containing dipeptide **5** was obtained from amino ester **9** by using the same peptide synthesis procedures as described above. The preparation of the l- and D-Phe-containing dipeptides **6** and **7** was carried out as reported earlier.[25] The ^{1}H- and ^{13}C NMR data for **1**−**7** are listed in Tables 2−4.

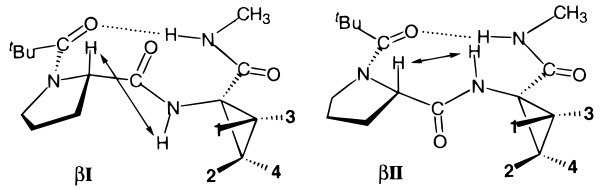

Figure 3. Schematic representation of a type I (left) and type II (right) β-turn for dipeptides **1**−**4** showing the anti (left) or syn (right) disposition of the Pro N−C^α and C′═O bonds, and the difference in the Pro-$C^\alpha H$/c_3Phe-N*H* interproton distance. Numbers **1**−**4** indicate the position of the phenyl ring in the c_3Phe-containing dipeptides as determined from the crystal structures of **1**, **2c**, and **3a**.

Piv-L-Pro-(2*R*,3*R*)c_3Phe-NHMe (1): R_f (CH_2Cl_2/*i*-PrOH 95/5) = 0.33. White solid (mp 221 °C). [α] = + 3.8 (*c* = 0.40, MeOH). IR (KBr) 3337, 3315, 1693, 1639, 1607, 1542, 1512 cm^{-1}. Anal. Calcd for $C_{21}H_{29}N_3O_3$: C, 67.90; H, 7.87; N, 11.31. Found: C, 67.78; H, 7.90; N, 11.35.

Piv-L-Pro-(2*S*,3*S*)c_3Phe-NHMe (2): R_f (CH_2Cl_2/*i*-PrOH 95/5) = 0.23. White solid (mp 270 °C). [α] = −288.6 (*c* = 0.42, MeOH). IR (KBr) 3344, 3268, 1695, 1637, 1604, 1551, 1527 cm^{-1}. Anal. Calcd for $C_{21}H_{29}N_3O_3$: C, 67.90; H, 7.87; N, 11.31. Found: C, 67.96; H, 7.85; N, 11.32.

Piv-L-Pro-(2*R*,3*S*)c_3Phe-NHMe (3): R_f (CH_2Cl_2/*i*-PrOH 95/5) = 0.28. White solid (mp 248 °C). [α] = −110.0 (*c* = 0.51, MeOH). IR (KBr) 3347, 3259, 1695, 1643, 1609, 1546 cm^{-1}. Anal. Calcd for $C_{21}H_{29}N_3O_3$: C, 67.90; H, 7.87; N, 11.31. Found: C, 68.00; H, 7.84; N, 11.27.

Piv-L-Pro-(2*S*,3*R*)c_3Phe-NHMe (4): R_f (CH_2Cl_2/*i*-PrOH 95/5) = 0.23. White solid (mp 84 °C). [α] = + 125.6 (*c* = 0.43, MeOH). IR (KBr) 3339, 3267, 1694, 1670, 1650, 1607, 1548 cm^{-1}. Anal. Calcd for $C_{21}H_{29}N_3O_3$: C, 67.90; H, 7.87; N, 11.31. Found: C, 67.81; H, 7.89; N, 11.35.

Piv-L-Pro-Ac_3c-NHMe (5): R_f (CH_2Cl_2/*i*-PrOH 9/1) = 0.41. White solid (mp 245 °C). [α] = −36.2 (*c* = 0.42, MeOH). IR (KBr) 3340, 3286, 1695, 1636, 1604, 1555, 1523 cm^{-1}. Anal. Calcd for $C_{15}H_{25}N_3O_3$: C, 60.99; H, 8.53; N, 14.23. Found: C, 60.86; H, 8.55; N, 14.28.

Piv-L-Pro-L-Phe-NHMe (6): R_f (CH_2Cl_2/*i*-PrOH 95/5) = 0.28. White solid (mp 145 °C). [α] = −70.8 (*c* = 0.61, MeOH). IR (KBr) 3344, 3282, 1677, 1646, 1603, 1538, 1518 cm^{-1}. Anal. Calcd for $C_{20}H_{29}N_3O_3$: C, 66.83; H, 8.13; N, 11.69. Found: C, 66.93; H, 8.12; N, 11.65.

Piv-L-Pro-D-Phe-NHMe (7): R_f (CH_2Cl_2/*i*-PrOH 95/5) = 0.27. White solid (mp 187 °C). [α] = −8.9 (*c* = 0.45, MeOH). IR (KBr) 3312, 3285, 1688, 1642, 1605, 1547, 1533 cm^{-1}. Anal. Calcd for $C_{20}H_{29}N_3O_3$: C, 66.83; H, 8.13; N, 11.69. Found: C, 66.75; H, 8.15; N, 11.73.

Z−L-Pro-(2*S*,3*S*)c_3Phe-NHMe (2c): R_f (AcOEt/CH_2Cl_2 7/3) = 0.46. White solid (mp 182 °C). [α] = −227.8 (*c* = 0.54, MeOH). IR (KBr) 3383, 3315, 1697, 1671, 1659, 1534 cm^{-1}. Anal. Calcd for $C_{24}H_{27}N_3O_4$: C, 68.39; H, 6.46; N, 9.97. Found: C, 68.48; H, 6.45; N, 9.93.

Boc-L-Pro-(2*R*,3*S*)c_3Phe-NHMe (3a): R_f (AcOEt/CH_2Cl_2 1/1) = 0.33. White solid (mp 244 °C). [α] = −150.0 (*c* = 0.40, MeOH). IR

Table 2. Proton Chemical Shifts for Piv-L-Pro-Xaa-NHMe in $CDCl_3$ (300 MHz, $c = 0.01$ M)[a]

		Pro				Xaa[b]							
peptide	*t*-Bu	$C^{\alpha}H$	$C^{\beta}H_2$	$C^{\gamma}H_2$	$C^{\delta}H_2$	NH	$C^{\alpha}H$	$C^{\beta}{}_{L}H_2$	$C^{\beta}{}_{D}H_2$	$C^{\delta}H$	$C^{\epsilon}H + C^{\zeta}H$	NH	CH_3
1	1.22	3.85	1.81	2.15/1.82	3.70	5.58		$1.59_c/2.12_t$	3.04_t	7.08−7.12	7.19−7.32	7.78	2.79
2	1.15	4.07	1.74/1.23	1.66/1.52	3.50/3.30	5.61		3.10_t	$1.51_c/2.04_t$	7.12−7.17	7.15−7.28	7.39	2.80
3	1.26	4.38	2.03	2.18/1.96	3.74	6.87		$1.33_c/2.27_t$	2.56_c	7.28−7.32	7.12−7.26	7.26	2.55
4	1.27	4.19	2.01	2.21/1.95	3.77	6.63		2.68_c	$1.28_c/2.18_t$	7.40−7.45	7.11−7.26	7.52	2.58
5	1.26	4.12	1.99/1.89	2.19/1.91	3.74	6.33		$1.02_c/1.62_t$	$0.84_c/1.48_t$			7.70	2.77
6	1.05	4.38	2.05/1.91	1.89	3.63/3.51	5.84	4.68	3.41/2.96		7.09−7.14	7.16−7.29	6.71	2.74
7	1.21	4.04	1.92	2.16/1.87	3.70	5.91	4.71		3.27/3.10	7.14−7.19	7.17−7.30	7.35	2.73

[a] The underlined resonances are significantly highfield shifted by ring current effect when comparing **1**−**4** with **5** and **6** with **7**. [b] The subscripts *c* and *t* specify the *cis* or *trans* disposition of the c_3Phe and Ac_3c cyclopropane protons with reference to the nitrogen atom. They have been assigned on the basis of the coupling constants ($J_{cis} > J_{trans}$) and of the perturbations introduced by the phenyl ring. $C^{\beta}{}_{L}$ and $C^{\beta}{}_{D}$ denote the β-carbon atom in the position corresponding to an L- and D-residue, respectively.

Table 3. Proton−Proton Vicinal (^3J) and Geminal (^2J) Coupling Constants for the Cyclopropane Ring in Dipeptides Piv-L-Pro-Xaa-NHMe **1**−**5**[a]

peptide	$^3J_{cis}$	$^3J_{trans}$	^2J_L	^2J_D
1	9.6	7.8	−5.7	
2	9.2	7.7		−5.6
3	9.8	8.4	−5.4	
4	10.1	8.6		−5.1
5	10.2	7.5	−4.2	−3.9

[a] Dispositions of the vicinal protons are specified by *cis* and *trans*. L and D denote the carbon atom in the position corresponding to an L- and D-residue, respectively.

(KBr) 3353, 3251, 1696, 1684, 1638, 1549 cm^{-1}. Anal. Calcd for $C_{21}H_{29}N_3O_4$: C, 65.10; H, 7.54; N, 10.84. Found: C, 65.21; H, 7.52; N, 10.80.

X-ray Diffraction. Single crystals of **1** (CH_2Cl_2 solvate), **2c**, and **3a** (CH_2Cl_2 solvate) were grown as indicated in Table 5. The X-ray diffraction data were collected on a Nonius CAD-4 four circle diffractometer, using graphite-monochromated Cu radiation (λ = 1.541 80 Å). The independent reflections were measured in the $\omega/2\theta$-scan mode and in the θ range 1−70°. Unique cell parameters were determined by least-squares refinement of the setting angles of 25 high angle reflections ($20° < \theta < 30°$). The main crystallographic data of the derivatives investigated in the present study are given in Table 5. The crystal structures were solved by direct methods using SIR92.[31] The E-maps revealed the whole molecules except the hydrogen atoms. Refinement of the structures was performed using SHELXL-93.[32] Heavy atoms were affected by anisotropic thermal factors, while the hydrogen atoms were located by calculation and affected by an isotropic thermal factor of 5 $Å^2$. The NH hydrogens were replaced at a distance of 1.03 Å from nitrogen in the direction found by refinement.[33] The residual R factors are indicated in Table 5. Crystal data, fractional coordinates for the hydrogen and non-hydrogen atoms, equivalent thermal parameters, and anisotropic temperature parameters for the non-hydrogen atoms, interatomic bond lengths and bond angles, and torsional angles have been deposited as Supporting Information.

^{1}H NMR and IR Spectroscopy. Structural analysis of compounds **1**−**7** in solution was performed by NMR and IR techniques. ^{1}H NMR spectra were obtained using a Bruker AC-200P and ARX-300 apparatus with TMS or the solvent signal as the internal reference, respectively. Peptide concentrations were 0.01 M. Proton resonances were assigned in $CDCl_3$ and DMSO-d_6 by COSY and HOHAHA experiments. Nuclear Overhauser enhancement due to the proximity of Pro-$C^{\alpha}H$/c_3Phe-N*H* was estimated using the ARX-300 apparatus through 1D-NOESY difference experiments by irradiation at the Xaa-N*H* frequency. The solvent accessibility of the amide protons, which is related to their free or hydrogen-bonded character, was investigated by considering the influence of changes in the DMSO-d_6 content in $CDCl_3$/DMSO-d_6 mixtures. The resonance of a free proton is rapidly shifted to low fields, whereas that of a hydrogen-bonded proton is only weakly affected by DMSO-d_6 N*H*-solvation.[25,34] IR spectra were obtained in the Fourier transform mode on a Bruker IFS-25 apparatus in order to investigate the *NH* (3200−3500 cm^{-1}) and *C′O* (1580−1720 cm^{-1}) stretching frequencies in CH_2Cl_2, MeCN, and DMSO. Peptide concentrations used were 0.005 M, and further dilution confirmed the absence of any molecular aggregation. A free secondary amide group exhibits an *NH* absorption at 3400−3450 cm^{-1} and a *C′O* absorption at 1650−1700 cm^{-1}, while the free urethane Boc/Z-*C′O* absorbs at 1700−1720 cm^{-1}. The tertiary nature of the Pro-preceding amide group, along with the presence of a quaternary carbon adjacent to the carbonyl, results in a very low frequency for the free Piv-*C′O* at about 1620 cm^{-1}, out of the usual region for peptide carbonyls.[25] The Pro-preceding pivaloyl group has another advantage; it prevents the Piv-Pro amide bond from assuming the *cis* conformation for steric reasons.[35] When engaged in an intramolecular hydrogen bond, both *NH* and *C′O* absorptions are shifted to lower wavenumbers. The contributions of the residual water in the solvent, if any, were eliminated by correction in the 3500−3600 cm^{-1} region where the peptide does not absorb.

Results and Discussion

Crystal Structures. The dichloromethane molecules in the solvates of both **1** and **3a** are thermally agitated, as are the *t*-Bu and Me terminal groups. The same is true for the c_3Phe phenyl carbons. The dimensions of the cyclopropane ring (Figure 4) are quite similar to those already found for the Ac_3c residue[17c] although the bond connecting the branched carbons is approximately 0.04 Å longer than the other two C−C bonds. As expected, the intracyclic bond angles are near to 60°, but the bond angle at the methylene carbon is a little larger than those at the other two branched carbons. We also note the short N−C^{α} and C^{α}−C′ bonds, which is in agreement with the conjugative ability of the cyclopropane ring, and the large N−C^{α}−C′ angle (117°), which greatly exceeds the standard value. The C^{β}−C^{γ} link between the cyclopropane and phenyl rings ranges from 1.46 Å in **2c** to 1.49 Å in **1** and **3a**, while the bond angles concerning the cyclopropane carbon bearing the phenyl ring are largely above 120°. The other bond lengths and bond angles in the dipeptides have expected values.

The main torsional angles are listed in Table 6. All three molecules are folded by an intramolecular *NH*(Me) to Piv-*C′O* hydrogen bond (Table 7) that closes a 10-membered pseudocycle typical of a β-turn.[36] We note the N···O distance of 3.15 Å in

(31) Altomare, A.; Cascarano, G.; Giacovazzo, C.; Guagliardi, A. *J. Appl. Crystallogr.* **1993**, *26*, 343−350.
(32) Sheldrick, G. M. *SHELXL 93, Program for the Refinement of Crystal Structures*; University of Göttingen: Germany, 1993.
(33) Taylor, R.; Kennard, O. *Acta Crystallogr., Sect. B* **1983**, *39*, 133−138.
(34) Pitner, T. P.; Urry, D. W. *J. Am. Chem. Soc.* **1972**, *94*, 1399−1400.
(35) (a) Nishihara, H.; Nishihara, K.; Uefuji, T.; Sakota, N. *Bull. Chem. Soc. Jpn* **1975**, *48*, 553−555. (b) Liang, G. B.; Rito, C. J.; Gellman, S. H. *Biopolymers* **1992**, *32*, 293−301.
(36) Rose, G. D.; Gierasch, L. M.; Smith, J. A. *Adv. Protein Chem.* **1985**, *37*, 1−109.

Table 4. ^{13}C Chemical Shifts for Piv-L-Pro-Xaa-NHMe in $CDCl_3$ (75 MHz, $c = 0.01$ M)[a]

	Piv			Pro					Xaa								
	CH_3	C	C′O	C^α	C^β	C^γ	C^δ	C′O	C^α	C^{β_D}	C^{β_L}	C^γ	C^δ	C^ϵ	C^ζ	C′O	CH_3
1	27.14	38.85	178.08	63.14	27.38	26.39	48.72	174.05	40.03	30.53	20.21	135.41	128.52	128.31	127.00	171.06	26.85
2	27.01	38.96	178.22	63.31	27.33	25.81	48.56	172.49	39.74	19.20	31.01	135.80	128.78	127.98	126.75	170.94	26.79
3	27.31	39.11	178.46	62.69	27.11	26.30	48.68	173.80	41.80	34.08	19.04	135.49	129.06	127.82	126.67	168.38	26.49
4	27.26	38.97	178.15	63.25	27.47	26.47	48.79	174.07	41.13	19.03	34.87	135.80	129.33	127.72	126.55	168.62	26.59
5	27.19	38.95	178.29	63.31	27.54	26.44	48.82	173.77	34.78	16.09	17.01					171.67	26.80
6	26.97	39.09	178.69	63.33	27.84	25.96	48.71	171.41	52.84		36.68	136.67	129.33	128.74	127.13	171.02	26.36
7	27.17	38.88	177.98	63.18	27.64	26.33	48.73	172.73	53.55	36.76		136.69	129.25	128.71	126.96	171.04	26.41

[a] C^{β_L} and C^{β_D} denote the β-carbon atom in the position corresponding to an L- and D-residue, respectively. They have been assigned by 2D $^1H-^{13}C$ heteronuclear zero and double quantum coherence correlation.

Table 5. Crystal Data

peptide	**1**[a]	**2c**[b]	**3a**[c]
crystal system	orthorhombic	monoclinic	orthorhombic
space group	$P2_12_12_1$	$P2_1$	$P2_12_12_1$
unit cell dimensions			
a, Å	9.542(1)	4.947(2)	10.127(1)
b, Å	9.918(2)	21.204(4)	13.033(3)
c, Å	26.268(6)	10.671(2)	19.130(3)
β, deg		99.33(3)	
Z	4	2	4
density$_{calcd}$, g·cm^{-3}	1.219	1.267	1.243
reflections collected	2550	2070	2537
independent reflections	2499 [$R_{int} = 0.079$]	2070 [$R_{int} = 0.000$]	2474 [$R_{int} = 0.076$]
data/restraints/parameters	2449/2/279	2070/2/287	2474/2/289
residual factors [$I > 2\,\sigma(I)$]	$R_1 = 0.055$, $wR_2 = 0.139$	$R_1 = 0.048$, $wR_2 = 0.120$	$R_1 = 0.062$, $wR_2 = 0.170$

[a] Single crystals of **1** (CH_2Cl_2 solvate) grown by slow diffusion of liquid petroleum ether in a CH_2Cl_2 solution. [b] Single crystals of **2c** grown by slow evaporation of a CH_2Cl_2/diisopropyl ether solution. [c] Single crystals of **3a** (CH_2Cl_2 solvate) grown by slow evaporation of a CH_2Cl_2 solution.

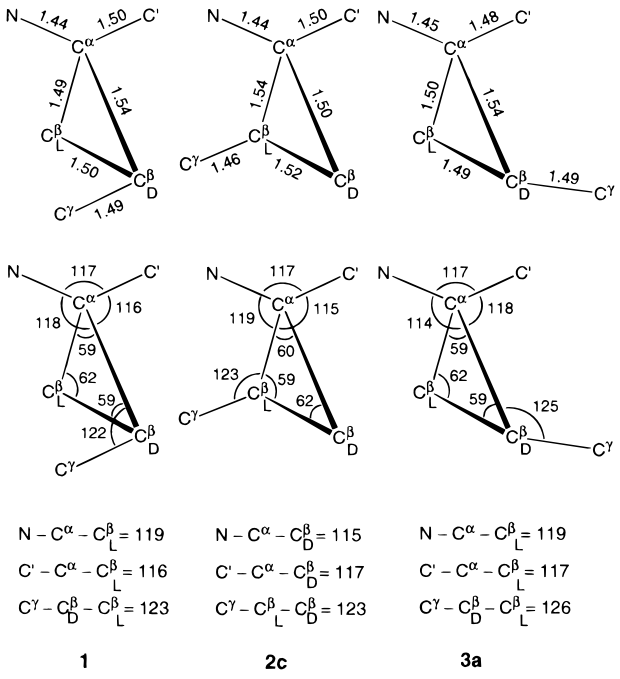

Figure 4. Bond distances (up) and bond angles (down) for the cyclopropane ring in the crystal molecular structures of **1**, **2c**, and **3a**. C^{β_L} and C^{β_D} denote the carbon atom in the position corresponding to an L- and D-residue, respectively.

2c, which is at the upper limit for hydrogen bonding[37] and larger than the corresponding distance in **1** (2.89 Å) and **3a** (2.87 Å). The orientation of the middle amide group, with the proline C′=O and $C^\alpha-H$ bonds in the anti disposition, corresponds to the type II β-turn (Figure 5), which has already been observed in the crystal molecular structure of Boc-Pro-Ac_3c-Gly-NH_2 and in homologous derivatives with larger cycloalkane rings.[17b] It is remarkable that all of the Ac_3c-containing oligopeptides crystallized thus far that are large enough to form a β-turn are actually β-folded. However, the turn is generally of type I,[17c] except for the tripeptide mentioned above.

Table 6. Main Torsional Angles (deg)

fragment	angle	**1**	**2c**	**3a**
Piv/Z/Boc	ω	177	178	−177
Pro	ϕ	−60	−51	−56
	ψ	134	134	131
	ω	−173	174	−175
c_3Phe	ϕ	89	72	77
	ψ	−5	0	11
	ω	−176	−174	−176
	χ^1	−4	8	−135
	χ^2	56/−127	−47/133	93/−90

The proline ring adopts the classical envelope C^γ-exo conformation in **1**, and the twisted C^β−endo/C^γ−exo conformation in **2c** and **3a**.[38] As expected,[35] the Piv group in **1** is transplanar. The participation of its carbonyl in the intramolecular hydrogen bond typical of the β-folded structure imposes the trans−trans conformation on the Z group[39] in **2c** and on the Boc group[40] in **3a**.

The molecules are connected by intermolecular hydrogen bonds between *NH* and *C′O* with typical N···O distances (Table 7).[37] Additionally, in both **1** and **3a**, one of the CH_2Cl_2 protons is in close contact with an amide oxygen. The two phenyl rings in **2c** are stacked in files.

(37) (a) Ramakrishnan, C.; Prasad, N. *Int. J. Pept. Protein Res.* **1971**, *3*, 209−231. (b) Taylor, R.; Kennard, O.; Versichel, W. *Acta Crystallogr., Sect. B* **1984**, *40*, 280−288. (c) Gorbitz, C. H. *Acta Crystallogr., Sect. B* **1989**, *45*, 390−395.

(38) Nair, C. M. K.; Vijayan, M. *J. Indian Inst. Sci., Sect. C* **1981**, *63*, 81−103.

(39) Benedetti, E.; Pedone, C.; Toniolo, C.; Dudek, M.; Némethy, G.; Scheraga, H. A. *Int. J. Pept. Protein Res.* **1983**, *21*, 163−181.

(40) Benedetti, E.; Pedone, C.; Toniolo, C.; Némethy, G.; Pottle, M. S.; Scheraga, H. A. *Int. J. Pept. Protein Res.* **1980**, *16*, 156−172.

Table 7. Dimensions (Å, deg) of the Hydrogen Bonds[a]

peptide	donor (D)	acceptor (A)	symmetry code	D···A	H···A	D−H···A
1	*NH*(Me)	Piv-*C′O*	*x*; *y*; *z*	2.89	2.01	141
	c_3Phe-*NH*	c_3Phe-*C′O*	$-x$; $-0.5+y$; $-0.5-z$	2.83	1.80	175
	CH_2Cl_2	Pro-*C′O*	$1+x$; *y*; *z*	3.10	2.15	167
2c	*NH*(Me)	Z-*C′O*	*x*; *y*; *z*	3.15	2.17	159
	c_3Phe-*NH*	Pro-*C′O*	$-1+x$; *y*; *z*	2.95	1.94	167
3a	*NH*(Me)	Boc-*C′O*	*x*; *y*; *z*	2.87	1.99	142
	c_3Phe-*NH*	c_3Phe-*C′O*	$0.5+x$; $1.5-y$; $-1-z$	2.79	1.77	174
	CH_2Cl_2	Pro-*C′O*	$0.5+x$; $0.5-y$; $-z$	3.09	2.44	125

[a] The NH hydrogens have been replaced at 1.03 Å from N in the direction found by refinement.[33]

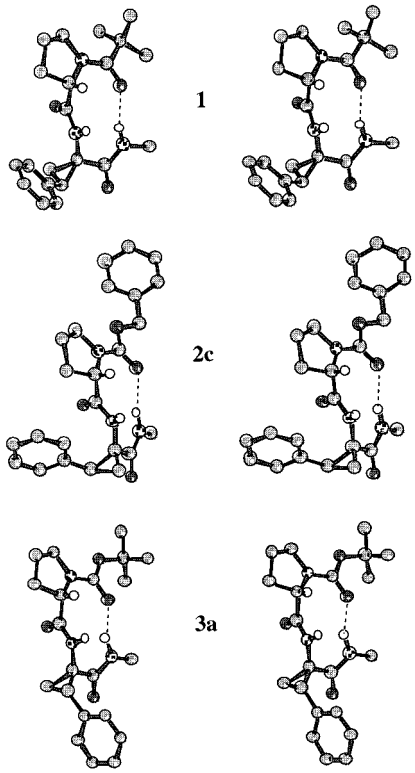

Figure 5. Stereoviews of the βII-folded crystal molecular structures of **1**, **2c**, and **3a**, indicating the intramolecular hydrogen bond.

Structures in Solution. The *NH* and *C′O* stretching frequencies for dipeptides **1**−**5** (Table 8) have been assigned by comparison with those for **6** and **7**,[25] and from the perturbation induced by Piv/Boc and NHMe/OMe exchange. They confirm the existence in CH_2Cl_2 of a strong intramolecular *NH*(Me) to Piv-*C′O* hydrogen bond that is typical of the β-turn structure. Thus, *NH*(Me) gives rise to an intense and broad *NH* stretching absorption at about 3350−3360 cm^{-1} (Table 8) and its proton resonance experiences a very small shift on going from $CDCl_3$ to DMSO-d_6 (Table 9). In comparison, the free c_3Phe-*NH* and Ac_3c-*NH* are characterized by a sharp IR absorption at about 3410−3425 cm^{-1} and a much higher solvent sensitivity of the proton resonance. This behavior is similar to that already reported for the homologous phenylalanine-containing dipeptides **6** and **7**.[25] However, the presence of an absorption at 3450 cm^{-1}, more intense for **6** than for **7** and corresponding to a free *NH*(Me) site, indicates the existence of a noticeable fraction of open molecules in these cases. This is confirmed by the higher sensitivity to solvent polarity observed for the N*H*(Me) proton resonance for **7** and, to a greater extent, for **6** (Table 9).

The Piv-*C′O* absorption, eventually corrected for residual water contribution, for derivatives **1**−**5** in CH_2Cl_2 (Table 8) is shifted to lower frequencies with reference to that observed at 1619 cm^{-1} for Piv-Pro-OMe, where it is free from any intramolecular interaction. One also notes its splitting into two components at about 1601 and 1612 cm^{-1}, with the relative intensities depending on the presence and orientation of the aromatic substituent (Figure 6). This indicates the occurrence of two different hydrogen-bonded states for this carbonyl group, which we believe to denote types I and II β-folded molecules. The same double contribution is observed for **7**, whereas **6** displays a single bonded absorption at 1611 cm^{-1} and a weaker free contribution at 1620 cm^{-1} (Table 8).

The type I and II β-turns differ essentially in the orientation of the middle amide bond (Figure 3). The absence of the Xaa-C$^{\alpha}$*H* proton from **1**−**5** precludes their discrimination by the $^3J_{NH-C\alpha H}$ coupling constant commonly used for the structural analysis of peptides.[41] Due to the existence of the second C$^{\beta}$ chiral center in **1**−**4** and the particular electronic hybridization state of the cyclopropane ring, circular dichroism, as proposed by Perczel et al.,[42] is also excluded. We therefore considered the Pro-C$^{\alpha}$*H*/Xaa-N*H* interproton distance, which is longer in the βI than in the βII-turn (Figure 3) and should be reflected by a weaker nuclear Overhauser enhancement (nOe) for the former. The Pro-C$^{\alpha}$*H*/Xaa-N*H* nOe in $CDCl_3$ has actually proven to be significantly smaller for **6** than for **7** (Table 10), and in CH_2Cl_2 solution, these compounds are known to essentially accommodate the βI- and βII-turns, respectively.[25] We therefore conclude that in CH_2Cl_2 the Piv-*C′O* frequency components at 1610−1615 and 1600−1605 cm^{-1} are effectively typical of the type I and type II β-turn, respectively. On this basis, the βI/βII ratio, estimated from the relative intensities of the Piv-*C′O* components in CH_2Cl_2 for all seven compounds, nicely correlates with the Pro-C$^{\alpha}$*H*/Xaa-N*H* nOe in $CDCl_3$ solution (Table 10).

It has already been pointed out that the βI- and βII-turns can also be discriminated by the Pro-*C′O* stretching frequency, which respectively translates the *anti* or *syn* orientation of the $(i+1)$ proline N−C$^{\alpha}$ and C′═O bonds (Figure 3).[25] The former gives rise to a lower frequency absorption (1685 cm^{-1} for **6**) than the latter (1692 cm^{-1} for **7**) (Table 8). Dipeptides **1**, **3**, and **4**, which essentially assume the type II β-turn (Table 10), present a single Pro-*C′O* absorption at a high frequency (about 1700 cm^{-1}), whereas **2**, which equally adopts the βI- and βII-turns, actually presents two Pro-*C′O* contributions at 1705 cm^{-1} (type II) and 1694 cm^{-1} (type I). The particular hybridization state of the c_3Phe α-carbon in **1**−**4** with reference to **6** and **7** is probably responsible for the higher Pro-*C′O* frequency in **1**−**4**.

In the absence of the phenyl ring, the βII-turn is the most favored structure for **5** in CH_2Cl_2. It has also been observed in the crystal structure of Boc-Pro-Ac_3c-Gly-NH_2,[17b] whereas other Ac_3c-containing peptides devoid of proline adopt the type I

(41) Bystrov, V. F. *Prog. Nucl. Magn. Reson. Spectrosc.* **1976**, *10*, 41−81.

(42) Perczel, A.; Hollósi, M.; Sándor, P.; Fasman, G. D. *Int. J. Pept. Protein Res.* **1993**, *41*, 223−236.

Table 8. Amide NH and C′O Stretching Frequencies (cm^{-1})[a] for Piv-L-Pro-Xaa-NHMe in CH_2Cl_2, MeCN, and DMSO Solutions ($c = 5 \times 10^{-3}$ M)

peptide/ solvent		*NH*(Me)		Piv-*C′O*			Pro-*C′O*		
	Xaa-*NH*, free	free	bonded	free	βI-bonded	βII-bonded	βI-free	βII-free	Xaa-*C′O*, free
1/CH_2Cl_2	3408[m]	*b*	3350[s]	*b*	1612[vw]	1601[s]		1701[s]	1658[s]
MeCN	——3347[c]——			*b*		1606[s]		1699[s]	1660[s]
DMSO	——3248[d]——		3340[s]	*b*		1604[s]		1693[s]	1657[s]
2/CH_2Cl_2	3424[m]/3413[m]	*b*	3360[s]	*b*	1612[m]	1601[m]	1694[m]	1705[m]	1660[s]
MeCN	3410[vw]	——3353[c]——		*b*		1605[s]		1702[s]	1660[s]
DMSO	——3248[d]——		3347[s]	*b*		1603[s]		1696[s]	1657[s]
3/CH_2Cl_2	3416[m]	*b*	3362[s]	*b*	1614[w]	1601[s]		1699[s]	1662[s]
MeCN	——3354[c]——			*b*		1606[s]		1697[s]	1664[s]
DMSO	——3246[d]——		3350[s]	*b*		1604[s]		1691[s]	1663[s]
4/CH_2Cl_2	3415[m]	*b*	3358[s]	*b*	1614[vw]	1602[s]		1699[s]	1658[s]
MeCN	——3353[c]——			*b*		1606[s]		1695[s]	1661[s]
DMSO	——3246[d]——		3348[s]	*b*		1604[s]		1689[s]	1659[s]
5/CH_2Cl_2	3420[m]	*b*	3352[s]	*b*	1612[w]	1601[s]		1700[s]	1655[s]
MeCN	——3350[c]——			*b*		1605[s]		1698[s]	1658[s]
DMSO	——3251[d]——		3340[s]	*b*		1604[s]		1692[s]	1655[s]
6/CH_2Cl_2	3428[vw]/3413[m]	3450[w]	3355[s]	1620[w]	1611[s]		1685[s]		1666[s]
MeCN	3430[vw]/3413[m]	——3355[c]——		1620[w]		1608[m]		1685[m]	1670[s]
DMSO	——3273[d]——		3337[m]	1619[m]		1604[m]		1685[m]	1667[s]
7/CH_2Cl_2	3419[m]	3450[vw]	3345[s]	*b*	1614[w]	1601[s]		1692[s]	1666[s]
MeCN	3425[w]	——3346[c]——		1620[vw]		1605[s]		1689[s]	1668[s]
DMSO	——3260[d]——		3328[s]	1619[w]		1603[s]		1684[s]	1666[s]

[a] Strong (s), medium (m), weak (w), and very weak (vw) absorption band. [b] The free absorption is not visible. [c] Broad absorption due to the superimposed MeCN-solvated free and intramolecularly bonded NHs. [d] Broad absorption denoting the DMSO-solvated free NHs.

Table 9. Chemical Shift and Solvent Sensitivity (ppm) of the Amide N*H* Proton Resonances for Piv-L-Pro-Xaa-NHMe ($c = 0.01$ M)

	Xaa-N*H*			N*H*(Me)		
peptide	$CDCl_3$	DMSO-d_6	$\Delta\delta^a$	$CDCl_3$	DMSO-d_6	$\Delta\delta^a$
1	5.58	7.99	2.41	7.78	7.81	0.03
2	5.61	8.65	3.04	7.39	7.70	0.31
3	6.87	8.89	2.02	7.26	7.59	0.33
4	6.63	8.83	2.20	7.52	7.75	0.23
5	6.33	8.66	2.33	7.70	7.84	0.14
6	5.84	7.65	1.81	6.71	7.68	0.97
7	5.91	8.28	2.37	7.35	7.91	0.56

[a] Shift of the N*H* proton resonance on going from $CDCl_3$ to DMSO-d_6.

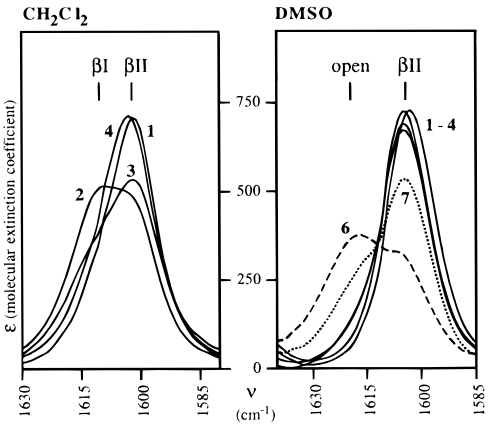

Figure 6. Piv-*C′O* absorption profile with assignment for derivatives **1**−**4** in CH_2Cl_2 (left) and **1**−**4**, **6**, and **7** in DMSO (right), showing the influences of the stereochemistry and the solvent on the βI/βII-turn ratio.

β-turn.[17c] In fact, proline is known to accommodate with a higher frequency than the other residues the conformation corresponding to ψ of about +150°,[43] a value typical of the βII-turn.

(43) MacArthur, M. W.; Thornton, J. M. *J. Mol. Biol.* **1991**, *218*, 397−412.

Table 10. Nuclear Overhauser Enhancement of the Pro-C$^{\alpha}$*H* Proton Resonance by Irradiation at the Xaa-N*H* Resonance for Piv-L-Pro-Xaa-NHMe. Comparison with the βI/βII Ratio in CH_2Cl_2 as Deduced from the Piv-*C′O* Absorption Profile

		nOe (%)		
peptide	Xaa	$CDCl_3$	DMSO-d_6	βI/βII[a] CH_2Cl_2
1	(2*R*,3*R*)c_3Phe	28	34	21/79
2	(2*S*,3*S*)c_3Phe	17	39	56/44
3	(2*R*,3*S*)c_3Phe	23	31	37/63
4	(2*S*,3*R*)c_3Phe	27	35	21 /79
5	Ac_3c	24	34	26/74
6	L-Phe	8	*b*	100/ 0
7	D-Phe	27	*b*	17/83

[a] Estimation from the relative intensities of the two components at about 1612 (βI-turn) and 1601 cm^{-1} (βII-turn) of the Piv-*C′O* absorption band (see Table 8 and Figure 6). [b] Not determined because of Pro-C$^{\alpha}$*H* and Phe-C$^{\alpha}$*H* resonance overlapping.

The βI/βII ratio varies with the orientation of the phenyl ring, which is dictated by cyclopropane chirality in **1**−**4**. The βII-turn is by far the most stable structure for both **1** and **4**, while the type I β-turn is present to a significant extent for **3** and even becomes the favored disposition for **2** (Table 10). Thus, the rigidity of the cyclopropane moiety, which fixes the phenyl orientation at χ^1 of about 0° for both dipeptides **1** and **2**, allows us to confirm the hypothesis previously proposed to explain the different folding preferences for **6** and **7** in CH_2Cl_2.[25] The π-orbitals of the aromatic ring are responsible for an attractive interaction with the c_3Phe-*NH* and for a repulsive interaction with the Pro-*C′O*, and both effects tend to favor the βI-turn for **2** and the βII-turn for **1** (Figure 3). As for **3** and **4**, the phenyl ring probably affects by repulsion the orientation of the c_3Phe-*C′O* with reference to the cyclopropane, and this may modulate to a smaller extent the βI/βII ratio, as indicated in Table 10.

The free Xaa-*NH* vibrator, which gives rise to a single absorption band for **1**, **3**−**5**, and **7**, exhibits a double absorption in the cases of **2** and **6** (Table 8). This splitting probably represents two different dispositions of the N−H bond with respect to the phenyl π-orbitals in relation with the βI/βII equilibrium for **2**, and the rotation of the Phe C$^{\alpha}$−C$^{\beta}$ bond in **6**.[25]

In DMSO, the *NH*(Me) stretching frequency for **1**−**5**, at about the same value as in CH_2Cl_2 (Table 8), confirms the hydrogen-bonded state of this vibrator, and this is in agreement with the very weak sensitivity of the N*H*(Me) proton resonance to DMSO-d_6 solvation (Table 9). The corresponding absorption in MeCN overlaps that of the solvated Xaa-*NH*. In both aprotic media, the low value of the Piv-*C′O* stretching frequency supports the retention of the β-folded structure. However, the existence of a single contribution at a low-frequency denotes the sole occurrence of the type II β-turn, and this is independent of the c_3Phe chirality (Figure 6). This is corroborated by the high Pro-C$^{\alpha}$*H*/c_3Phe-N*H* or Ac$_3$c-N*H* nOe value in DMSO-d_6 (Table 10), which provides evidence of a change in the folding mode with reference to that observed in $CDCl_3$. We note that the folded conformers of the D-Phe-containing dipeptide **7** and, to a greater extent, of the L-Phe derivative **6** are much more sensitive to DMSO solvation than those of the cyclopropane dipeptides **1**−**5** (Table 8), a fact revealed by the absorption at about 1619 cm^{-1}, which is typical of the free Piv-*C′O* site in Piv-Pro-OMe.

DMSO is a strong solvating aprotic medium and tends to interact with the free Xaa-*NH* site, which is in fact less accessible in the βI-turn, where it is directed toward the inner part the molecule, than in the βII-turn, where it points outward (Figure 3). This is probably the reason why all the cyclopropane-containing dipeptides **1**−**5** adopt the same βII disposition and why the folded conformation of **6** becomes of the βII-type, under the above conditions. A supporting argument is provided by the βII-folded crystal molecular structures of **1**, **2c**, **3a** (Table 7), and **6**,[25] where the Xaa-*NH* is hydrogen-bonded to an amide carbonyl of a neighboring molecule. These results indicate that NH solvation or intermolecular interactions are able to compensate for the energy difference between type I and II β-turns, even in the cases of **2** and **6** where the βI-turn is stabilized by the Xaa-*NH*/aromatic ring attractive interaction.

Conclusion

The Pro-c_3Phe dipeptide sequences investigated in the present study exhibit a high tendency to β-folding in solution, even in DMSO, which is a strong solvating medium where the homologous peptides with a linear side chain adopt open conformations to a much larger extent. This fact confirms the tendency of the cyclopropane ring to favor a zero value for the ψ torsional angle, a prerequesite for β-folding.[17c]

The β-folding mode for the above derivatives, containing the c_3Phe residue in the so-called $i + 2$ position, depends on the solid or solution state, on the nature of the solvent, and on the stereochemistry of the cyclopropane ring. In weakly polar media, the βI- and the βII-turns coexist in a ratio that varies with phenyl orientation, while in DMSO solution and in the solid state, where solvation or molecular packing play an important role, all of them accommodate the βII-folded conformation.

The βI- and βII-turns can be distinguished by the Piv-*C′O* stretching frequency, and the IR results are in good quantitative correlation with the Pro-C$^{\alpha}$*H*/Xaa-N*H* nOe magnitude. This agreement allows us to conclude that both techniques constitute reliable methods to distinguish the βI- and βII-folding modes in peptides incorporating α,α-disubstituted amino acids, in which the Xaa $^3J_{NH-C\alpha H}$ is not present.

The present work illustrates the influence of the side chain orientation on the conformation of the peptide backbone. This point is of particular interest in the design of potent biologically active peptide derivatives using χ^1-constrained amino acid residues. The structural analysis of model peptides containing other constrained phenylalanine analogues is in progress.

Acknowledgment. The authors are grateful to Dr. M. D. Díaz-de-Villegas for her contribution to the NMR analysis and to Drs. C. Didierjean and A. Vicherat for technical assistance. Financial support from the Ministerio de Educación y Cultura (postdoctoral fellowship for A.I.J. and acción integrada HF 96-87), and Ministère des Affaires Etrangères (action intégrée 97039) is gratefully acknowledged.

Supporting Information Available: Crystal data, fractional coordinates for the hydrogen and non-hydrogen atoms, equivalent thermal parameters and anisotropic temperature parameters for the non-hydrogen atoms, interatomic bond lengths and bond angles, and torsional angles (21 pages, print/PDF). An X-ray crystallographic file, in CIF format, is available through the Web only. See any current masthead page for ordering information and Web access instructions.

JA9807439